Mineralogical Magazine, October 2015, Vol. 79(5), pp. 1203–1211

Yeomanite, $Pb_2O(OH)Cl$, a new chain-structured Pb oxychloride from Merehead Quarry, Somerset, England

R. W. Turner[1,*], O. I. Siidra[2], M. S. Rumsey[3], Y. S. Polekhovsky[4], Y. L. Kretser[5], S. V. Krivovichev[2], J. Spratt[3] and C. J. Stanley[3]

[1] The Drey, Allington Track, Allington, Salisbury SP4 0DD, Wiltshire, UK
[2] Department of Crystallography, Geological Faculty, St Petersburg State University, University Embankment 7/9, St Petersburg 199034, Russia
[3] Department of Earth Sciences, Natural History Museum, Cromwell Road, London SW7 5BD, UK
[4] Department of Mineral Deposits, St Petersburg State University, University Embankment 7/9, 199034 St Petersburg, Russia
[5] V. G. Khlopin Radium Institute, Roentgen Street 1, 197101 St Petersburg, Russia

[*Received 27 June 2014; Accepted 13 January 2015; Associate Editor: S. J. Mills*]

ABSTRACT

Yeomanite, $Pb_2O(OH)Cl$, is a new Pb-oxychloride found in the manganese pod mineral assemblage at Merehead (Torr Works) Quarry, near Cranmore, Somerset, England. Yeomanite is named in joint recognition of Mrs Angela Yeoman (1931–) and her company, Foster Yeoman, who operated Merehead Quarry for aggregate until 2006. The mineral is normally white, occasionally grey, with a white streak and a vitreous to transparent lustre. Invariably intimately associated with mendipite, yeomanite appears to be formed of small, twisted, rope-like fibres growing from the end of columnar mendipite masses, forming loose mats and strands resembling asbestos. Individual fibres are generally <8 mm long, but exceptionally may reach up to 15 mm. There is a perfect cleavage parallel to the long axis of the fibres but this is masked by the fibrous nature, especially as individual fibres break easily. The D_{calc} for the ideal formula is 7.303 g/cm^3. The mean RI in air at 589 nm is 2.27. The eight strongest reflections in the powder X-ray diffraction pattern [(*d* in Å) (*Intensity*) (*hkl*)] are: 2.880(100)(113); 2.802(78)(006); 3.293(61)(200); 3.770(32)(011); 2.166(22)(206); 1.662(19)(119); 2.050(18)(303); 3.054(17)(105) Yeomanite is orthorhombic, *Pnma*, $a = 6.585(10)$, $b = 3.855(6)$, $c = 17.26(1)$ Å, $V = 438(1)$ Å^3, $Z = 4$. Yeomanite is a new example of the growing family of lead oxychloride minerals that have a structure based upon oxocentred OPb_4 tetrahedra, which, in this mineral, jointly with $OHPb_3$ triangles, form $[O(OH)Pb_2]^+$ chains similar to those observed in synthetic $Pb_2O(OH)I$. Yeomanite is structurally related to sidpietersite, penfieldite and laurionite.

Keywords: yeomanite, new mineral, Pb oxyhalide, oxocentred units, crystal structure, Merehead quarry.

Introduction

For some time, the authors have been investigating the mineralogy of the Mendip Hills with particular reference to the assemblages of Pb oxychlorides and other Pb secondary minerals contained within the manganese pods that occur there, as well as similar oxychloride occurrences elsewhere in the world including Långban in Sweden, the Kombat mine in Namibia, the Mammoth St. Antony mine in Tiger, Arizona and the Kunibert mine in Rhine-Westphalia (see e.g. Turner, 2006; Rumsey 2008; Siidra *et al*. 2008; Krivovichev *et al*. 2009; Turner and Rumsey, 2010; Rumsey *et al*. 2011; Turner *et al*. 2012*a*; Williams *et al*., 2012, Siidra *et al*., 2013*a*,*b*).

The origin of the manganese oxide pods and the lead oxychloride phases that they enclose has been debated for many years. Turner (2006) suggested that all the lead oxychlorides were formed when galena deposits in Carboniferous limestones were locally exposed to seawater. Surface oxidation of

* E-mail: rturner@imbuia-holdings.com
DOI: 10.1180/minmag.2015.079.5.14

the galena initiated the deposition of manganate phases such as todorokite, which in turn adsorbed heavy metals from sea water and the local environment. A later hydrothermal event caused the galena to decompose, a variety of secondary minerals to form and conversion of the early Mn-rich manganate material to denser manganese oxides. These formed an impervious layer around the lead-rich core, creating a closed system. As temperatures fell, a range of minerals including the lead oxychloride-dominated assemblage formed. Being closed, each system can have a unique chemistry dependent only on local starting conditions, and thus we see considerable variance in mineralogy from pod to pod.

The most abundant oxychloride mineral in the assemblage is mendipite $Pb_3Cl_2O_2$ (Spencer, 1923). Chloroxiphite $Pb_3CuO_2(OH)_2Cl_2$ (Siidra *et al.,* 2008), diaboleite $Pb_2Cu(OH)_4Cl_4$ (Cooper and Hawthorne, 1995) and paralaurionite Pb(OH)Cl occur in, and often entirely enclosed by, mendipite, and are usually also accompanied by malachite, cerussite and 'hydrocerussite', and occasionally by mimetite and/or wulfenite. Other oxychloride minerals such as mereheadite $Pb_{47}O_{24}(OH)_{13}Cl_{25}(BO_3)_2(CO_3)$ (Krivovichev *et al.,* 2009), parkinsonite $Pb_7MoO_9Cl_2$ (Welch and Lepore, 2010), symesite $Pb_{10}(SO_4)O_7Cl_4.(H_2O)$ (Welch *et al.*, 2000), rickturnerite $Pb_7O_4[Mg(OH)_4](OH)Cl_3$, (Rumsey *et al.*, 2011) and rumseyite $[Pb_2OF]Cl$ (Turner *et al.*, 2012*b*) also occur in this environment, but are exceedingly rare, as is the oxycarbonate mineral plumbonacrite $Pb_5O(OH)_2(CO_3)_3$ which occurs with rickturnerite (Williams *et al*., 2012).

Aside from a thin rim of calcite lining the outermost edges, any cavity containing mendipite is invariably completely filled by a single mendipite crystal individual, which displays cleavage and parting planes giving rise to a columnar appearance. However, in the mid-1970s a small number of specimens of mendipite that had a strikingly different appearance were found in the #1 vein at Merehead quarry. In these specimens, mendipite did not completely fill the cavity in the manganese oxides, there were small voids in the mendipite itself, and the ends of the otherwise typical mendipite crystal individuals that adjoined these voids had a distinctly fibrous appearance, resembling that of asbestos (Figs 1, 2). This fibrous material has now been determined to consist of yeomanite. This material has not been seen since the original discovery, and with the knowledge that we now have, it seems likely that the occurrence

FIG. 1. The type specimen of yeomanite, showing the distinctive fibrous appearance. Scale bar in mm.

represented another 'micro-environment' (see Turner, 2006) that provided the specific conditions necessary for the formation of yeomanite. Since then, similar micro-environments have yielded other one-off finds, including the original find of (pink) symesite, and most recently, of rickturnerite and plumbonacrite (Williams *et al*., 2012).

Although known for many years, previous studies of what was then termed 'fibrous mendipite' were inconclusive. This was partly due to a lack of material and partly due to its fibrous nature, the latter leading to poor results from single-crystal X-ray studies. The problems were also compounded by significant variability in chemical analyses. We have now found that the material contains variable amounts of other admixed minerals including paralaurionite and mendipite, and this undoubtedly explains the variability in chemistry and powder X-ray data obtained in earlier studies.

FIG. 2. Scanning electron microscopy image of yeomanite fibres. The twisted, rope-like appearance can be seen clearly.

https://doi.org/10.1180/minmag.2015.079.5.14 Published online by Cambridge University Press

Yeomanite is named in joint recognition of Mrs Angela Yeoman (1931–) and her company, Foster Yeoman Ltd, who operated Torr Works (Merehead) Quarry for aggregate until 2006. Mrs Yeoman took a personal interest in mineral collecting, conservation and research work at Merehead and her company actively supported these activities for nearly 50 years. In addition to allowing access to the quarry, practical assistance was often provided in the form of heavy earth-moving plant to excavate newly exposed manganese pods or veins, and interesting material found when researchers were not present was frequently removed by company staff and stockpiled for later investigation. As a direct result of this cooperation, it has been possible to study the highly unusual manganese pod mineralization *in situ* and in considerable detail for some decades. This is now reflected in the number of mineral species identified from the quarry, ~70, of which ~15 are unusual Pb oxychloride or oxycarbonate minerals (Turner and Rumsey, 2010). Merehead Quarry is the type locality for six of these (mereheadite, parkinsonite, rickturnerite, rumseyite, symesite and the new mineral described here, yeomanite) and is now also the neotype locality for plumbonacrite (Rumsey *et al.,* 2014).

The holotype specimen of yeomanite shown in Fig. 1 is stored in the collections of the Natural History Museum, Cromwell Road, London SW7 5BD, UK, under catalogue number BM 2013,5. A co-type specimen is stored in the collections of the Smithsonian Institution in Washington, DC.

Occurrence and appearance

Yeomanite occurs in the Torr Works (Merehead) Quarry, East Cranmore, Somerset, UK. It is associated intimately with mendipite, which occurs filling cavities within the small dispersed masses of manganese and iron oxide material that form what are locally termed 'manganese pods'. Other oxychloride minerals found in the manganese pods include chloroxiphite, an as yet undescribed Co-rich variant of chloroxiphite, diaboleite, mereheadite, paralaurionite, parkinsonite, symesite, rickturnerite and rumseyite. Other Pb and Cu minerals, including mimetite, wulfenite, cerussite, 'hydrocerussite', malachite and 'crednerite' also occur in the same environment. Gangue minerals associated with mineralized manganese pods include aragonite, calcite and baryte. Undifferentiated pod-forming Mn oxides are typically a mixture of manganite and pyrolusite, associated with Fe oxyhydroxides such as goethite (Turner, 2006).

Yeomanite usually appears to be formed of small, twisted, rope-like fibres growing from the end of columnar mendipite masses. Yeomanite fibres form loose mats and strands, resembling asbestos (Fig. 1) in appearance. Individual fibres reach no more than 15 mm long, and are generally <8 mm. Under magnification (Fig. 2) the rope-like yeomanite fibres can be seen to be composed of twisted aggregates of minute hair-like crystals. Yeomanite fibres are brittle and where they have become detached from their mendipite matrix, loose masses of yeomanite are formed. Yeomanite is usually white and occasionally pale grey, with a white streak and a vitreous to transparent lustre. It is not fluorescent. The habit is fibrous, so it is not possible to determine crystal forms. No twinning was observed.

Physical Properties

Yeomanite has a Vickers Hardness Number (VHN_{20}) of 54.5 kg mm^{-2} ($n = 2$) and a Mohs hardness in the range ~½–2, but this latter is impossible to determine accurately due to the fibrous nature of the material. For the same reason, neither the tenacity nor the fracture could be determined, and it was also not possible to determine the precise crystallographic orientation of the perfect cleavage that is aligned with the long axis of the fibres.

Density could not be measured because of paucity of available material and its fibrous nature, but $D_{calc} = 7.303$ g cm^{-3} from the empirical formula.

Optical Properties

The material is non-metallic, but has a high RI typical of lead oxychlorides and has been studied using the methods common for metallic minerals to avoid using toxic RI liquids. In reflected light, yeomanite is light-grey to grey with white internal reflections. It is not pleochroic, and no bireflectance was observed due to the abundance of internal reflections but should be distinct according to the quantitative measurements presented in Table 1. Refractive indices calculated from the Fresnel equations (assuming $k = 0$) at 589 nm are 2.15 and 2.39 respectively for $R1$ and $R2$ (=R_{min} and R_{max}) yielding a mean of 2.27. The anisotropism $\Delta R_{589} = 3.58\%$. Reflectance measurements were made using a SiC standard in air in the range 400–700 nm (Table 2).

https://doi.org/10.1180/minmag.2015.079.5.14 Published online by Cambridge University Press

TABLE 1. Reflectance values of an unoriented section free of internal reflections on a measured area of 10 μm × 10 μm (SiC standard, measured in air) for yeomanite.

λ/nm	R_{max} %	R_{min} %
400	20.2	16.0
420	19.5	15.4
440	18.9	15.0
460	18.6	14.7
470	**18.4**	**14.5**
480	18.2	14.4
500	17.8	14.1
520	17.5	13.9
540	17.3	13.7
546	**17.2**	**13.7**
560	17.1	13.5
580	16.9	13.3
589	**16.8**	**13.3**
600	16.8	13.2
620	16.7	13.1
640	16.6	13.0
650	**16.6**	**12.9**
660	16.6	12.8
680	16.5	12.8
700	16.4	12.8

Wavelengths required by the Commission on Ore Mineralogy are given in bold.

Chemical Composition

Twenty analyses were performed on three different crystals checked previously by single-crystal X-ray using a Camscan-4DV scanning electron microscope and an AN-10000 semiconductor spectrometer at 30 kV and 0.7 nA at the Radium Institute, St Petersburg. The analytical lines Pb*Lα* and Cl*Kα* were used. The spectrum of the Pb*Mα* line was subtracted because of its overlap with the Cl*Kα* line. All calculations were made using *AF4/FLS* software provided by LINK systems. No elements other than those listed in Table 2 were detected. The hydroxyl component was calculated on the basis of structural considerations as insufficient sample exists for determination *via* CHN and/or any other analytical technique. The empirical formula (calculated on the basis of 3 anions per formula unit) is $Pb_{1.99}O_{0.98}(OH)_{1.01}Cl_{1.01}$. The simplified formula of yeomanite is $Pb_2O(OH)Cl$, which requires PbO 92.45, Cl 7.34, H_2O 1.87, O = Cl–1.66, total 100.00 wt.%.

TABLE 2. Chemical composition (wt.%) of yeomanite.

Constituent	wt.%	Range	SD	Probe Standard
PbO	92.3	91.97–92.50	0.4	Pyromorphite
Cl	7.4	7.35–7.48	0.1	Pyromorphite
H_2O*	1.9			
O = Cl	–1.7			
Total	99.9			

*Calculated on the basis of the crystal-structure data.

TABLE 3. Powder X-ray diffraction data for yeomanite.

I_{rel}	d_{obs}	d_{calc}	*h*	*k*	*l*
9	8.628	8.630	0	0	2
7	6.114	6.152	1	0	1
9	5.246	5.235	1	0	2
2	4.340	4.333	1	0	3
32	**3.770**	**3.762**	**0**	**1**	**1**
11	3.605	3.609	1	0	4
61	**3.293**	**3.293**	**2**	**0**	**0**
12	3.267	3.267	1	1	1
11	3.241	3.234	2	0	1
5	3.098	3.104	1	1	2
4	3.077	3.076	2	0	2
17	**3.054**	**3.057**	**1**	**0**	**5**
100	**2.880**	**2.880**	**1**	**1**	**3**
78	**2.802**	**2.877**	**0**	**0**	**6**
4	2.617	2.618	2	0	4
6	2.493	2.504	2	1	0
11	2.471	2.478	2	1	1
10	2.414	2.405	2	1	2
8	2.180	2.178	3	0	1
22	**2.166**	**2.166**	**2**	**0**	**6**
15	2.165	2.166	2	1	4
7	2.080	2.077	0	1	7
18	**2.050**	**2.051**	**3**	**0**	**3**
14	1.928	1.928	0	2	0
6	1.900	1.896	3	1	1
13	1.811	1.811	3	1	3
9	1.663	1.663	2	2	0
19	**1.662**	**1.662**	**1**	**1**	**9**
11	1.602	1.601	0	2	6
7	1.491	1.491	4	1	2
4	1.486	1.486	4	0	5
5	1.440	1.440	2	2	6
2	1.438	1.438	0	0	12
6	1.445	1.437	0	2	8

Strongest lines given in bold.

https://doi.org/10.1180/minmag.2015.079.5.14 Published online by Cambridge University Press

TABLE 4. Crystallographic data and refinement parameters for yeomanite.

Crystal size (mm)	0.18 × 0.001 × 0.001
Space group	*Pnma*
a (Å)	6.585(10)
b (Å)	3.855(6)
c (Å)	17.26(3)
V (Å^3)	438.1(12)
μ (mm^{-1})	77.182
D_{calc} (g cm^{-3})	7.304
Radiation wavelength (Å)	0.71073 (Mo*K*α)
θ-range (°)	2.36–25.37
Total no. of reflections	1700
Unique Reflections	415
Unique $\|F_o\| \geq 4\sigma_F$	329
R_{int}	0.19
R_1	0.106
R_1 (all data)	0.130
Goof	1.194
$\rho_{max,min}$ (e·Å^{-3})	+10.916/–6.038

Powder X-ray diffraction data

Preliminary powder X-ray measurements revealed that yeomanite forms intergrowths with paralaurionite. Thus it was decided to hand pick 20 homogenous fibrous crystals of yeomanite under the microscope. These were subsequently crushed and mounted in an epoxy ball on a glass fibre. Powder X-ray diffraction data were obtained using a Stoe Image Plate Diffraction System II at the Department of Crystallography, St Petersburg State University. Data (in Å for Mo*K*α) are listed in Table 3. Unit-cell parameters refined from the powder data are as follows: *Pnma, a* = 6.58(1) Å, *b* = 3.86(1) Å, *c* = 17.23(3) Å, *V* = 437(1) Å^3, *Z* = 4. The eight strongest reflections in the powder X-ray diffraction pattern [(*d* in Å) (*Intensity*) (*hkl*)] are: 2.880(100)(113), 2.802(78)(006), 3.293(61)(200), 3.770(32)(011), 2.166(22)(206), 1.662(19)(119), 2.050(18)(303), 3.054(17)(105)

Crystal structure

Analytical Procedure

Yeomanite forms asbestos-like mats of intergrown crystals, which diffract rather poorly under the X-ray beam. Consequently, 11 different crystals were independently checked to ensure that results

TABLE 5. Atomic coordinates and displacement parameters (Å^2) for yeomanite.

Atom	B.V.S.**	*x/a*	*y/b*	*z/c*	U_{eq}	U^{11}	U^{22}	U^{33}	U^{23}	U^{13}	U^{12}
Pb(1)	1.84	0.2683(4)	¾	0.01645(19)	0.0171(13)	0.0062(17)	0.011(3)	0.0346(19)	0.000	0.000(1)	0.000
Pb(2)	1.90	0.6862(5)	¾	0.17093(17)	0.0181(13)	0.0091(19)	0.012(3)	0.0334(18)	0.000	–0.002(1)	0.000
Cl(1)	0.60	0.330(4)	¼	0.1683(12)	0.028(6)	0.035(14)	0.015(18)	0.035(11)	0.000	0.002(9)	0.000
O(1)*	2.01	0.6106	¾	0.0506	0.050	0.050	0.050	0.050	0.000	0.000	0.000
OH(2)*	1.14	0.1415	¾	–0.1248	0.050	0.050	0.050	0.050	0.000	0.000	0.000

*Fixed during refinement; **bond-valence sum.

https://doi.org/10.1180/minmag.2015.079.5.14 Published online by Cambridge University Press

TABLE 6. Selected interatomic distances in the crystal structure of yeomanite.

Pb(1)–O(1)	2.330(4)
Pb(1)–O(1)	2.385(3) × 2
Pb(1)–OH(2)	2.576(5)
Pb(1)–Cl(1)	3.278(18) × 2
Pb(2)–O(1)	2.136(5)
Pb(2)–OH(2)	2.375(3) × 2
Pb(2)–Cl(1)	3.04(2) × 2
Pb(2)–Cl(1)	3.51(2) × 2

were consistent. The nature of the material meant that no individual yeomanite crystal that could provide a 'perfect' single-crystal study was found. The results reported here were obtained from the best one. We have also tried to measure yeomanite crystals by means of synchrotron radiation at the Swiss-Norwegian beamline, European Synchrotron Radiation facility (ESRF), Grenoble. However, the synchrotron data did not provide any improvement against laboratory data collected by means of microfocus tube radiation.

Details of the data collection and structure refinement are provided in Table 4. A very thin, needle-like crystal (0.18 mm × 0.001 mm × 0.001 mm) was mounted on a Bruker APEX II DUO X-ray diffractometer with a micro-focus X-ray tube operating with Mo$K\alpha$ radiation at 50 kV and 40 mA. These data were integrated and corrected for absorption using a multi-scan model and the Bruker programs *APEX* and *SADABS*. More than a hemisphere of data was collected with frame widths of 0.3° in ω, and with 280 s counting time per frame. The structure was first solved in the triclinic space group $P\bar{1}$. The obtained structure model was transformed into a monoclinic one using the *ADDSYM* algorithm incorporated in the *PLATON* program package (le Page, 1987; Spek, 2003). Then the monoclinic model was transformed to the orthorhombic model with the space group *Pnma*. The structure was finally solved by direct methods and refined to $R_1 = 0.106$ for 329 unique

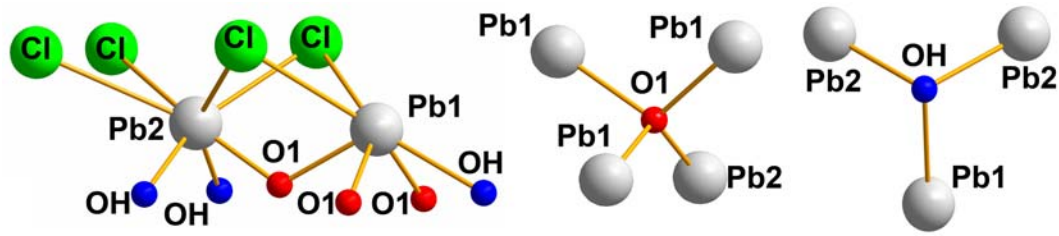

FIG. 3. Coordination of atoms in the crystal structure of yeomanite.

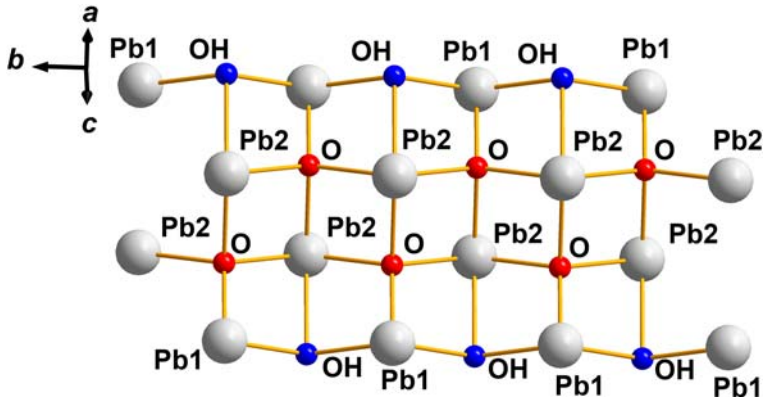

FIG. 4. The $[O(OH)Pb_2]^+$ chains in the crystal structure of yeomanite.

https://doi.org/10.1180/minmag.2015.079.5.14 Published online by Cambridge University Press

observed reflections. The difference Fourier electron density map displayed a series of high residual peaks (up to 10.916 e Å^{-3}) located close to the positions of the Pb atoms. We assign these peaks to the poor quality of the diffraction data collected on a yeomanite fibrous crystal. All of the atomic sites were checked to confirm that they were occupied fully. Positions of H atoms could not be localized. The final model included anisotropic displacement parameters for all the cations. The final atomic coordinates and displacement parameters are given in Table 5; selected interatomic distances are in Table 6. Bond-valence analysis was calculated using bond-valence parameters taken from Krivovichev and Brown (2001) for the Pb^{2+}–O bonds and from Brese and O'Keeffe (1991) for other bonds.

Structure description

Generally, the structure of yeomanite is similar to that recently described for the synthetic compound $Pb_2O(OH)I$ (Siidra *et al.*, 2013). The coordination environments of both Pb(1) and Pb(2) atoms (Fig. 3 and Table 6) clearly indicate stereochemical activity of the lone electron pairs on the Pb^{2+} cations. Because of the large size and variability of coordination polyhedra around Pb^{2+} cations and the high strength of *Me*–O, *Me*–OH bonds in

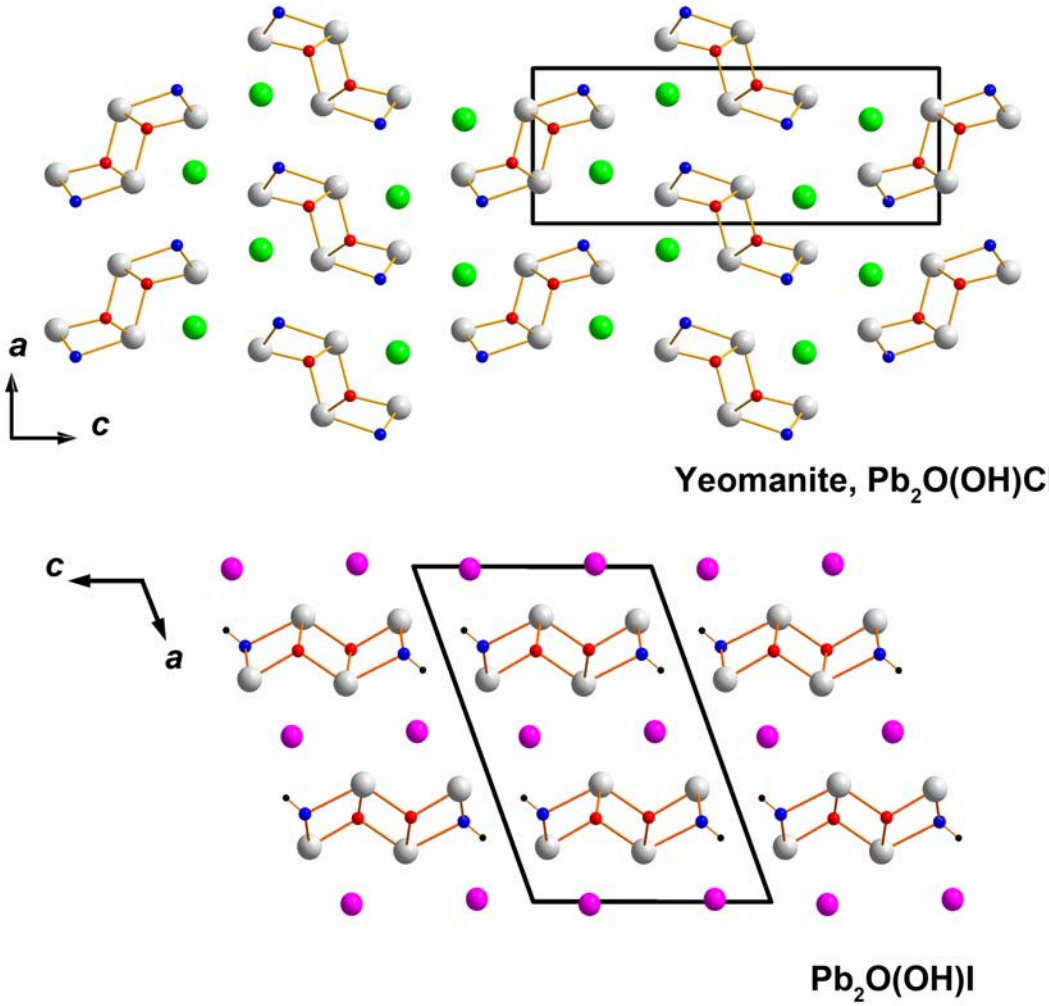

FIG. 5. Projections of the crystal structure of yeomanite (above) and $Pb_2O(OH)I$ (below) along the *b* axis.

https://doi.org/10.1180/minmag.2015.079.5.14 Published online by Cambridge University Press

comparison to *Me*–Cl bonds (*Me* = metal), it is convenient to describe the structure of yeomanite in terms of oxocentred OPb_4 tetrahedra (Krivovichev *et al.*, 2013) and hydroxocentred $OHPb_3$ triangles. The structure contains two symmetrically independent O atoms. Atom O(1) is tetrahedrally coordinated by four Pb^{2+} cations forming relatively short and strong O–Pb bonds. The mean O–Pb length in the $O1Pb_4$ tetrahedron is 2.31 Å, which is typical for such units. The OPb_4 tetrahedra link together *via* common edges and corners to form $[OPb_2]^{2+}$ chains (Fig. 4). Atom O(2) belongs to a hydroxyl group and its valence requirements are strongly influenced by the formation of the O–H bond (Table 6). Oxygen atoms belonging to hydroxyl groups are attached additionally to the $[OPb_2]^{2+}$ chains, thus forming novel one dimensional $[O(OH)Pb_2]^{+}$ units, previously unobserved for lead oxychloride minerals. The chains are parallel to the *b* axis and occur in both parallel and mutually perpendicular orientations. It is interesting that, in the structure of synthetic $Pb_2O(OH)I$, topologically identical chains occur only in parallels (Fig. 5). The positively charged $[O(OH)Pb_2]^{+}$ chains are linked one to another *via* rather weak Pb–Cl bonds, thus providing the 3D integrity of the crystal structure (Fig. 5).

Discussion

The structure of yeomanite is a new example of a lead oxychloride mineral based upon the $[O(OH)Pb_2]^{+}$ chains previously only reported for synthetic $Pb_2O(OH)I$. A short review of all minerals and synthetic compounds based on chains formed by OPb_4 tetrahedra and/or $OHPb_3$ triangles is provided by Siidra *et al.* (2013*c*). Yeomanite is most closely related to sidpietersite (Cooper and Hawthorne, 1999), penfieldite (Merlino *et al.*, 1995) and laurionite (Venetopoulos and Rentzeperis, 1975). It is noteworthy that the formula '$Pb_2O(OH)Cl$' was first suggested by Welch *et al.* (1998) for mereheadite. However, structural solution of the crystal structure of mereheadite by Krivovichev *et al.* (2009) demonstrated that it is actually a complex lead carbonate-borate oxychloride mineral with the chemistry $Pb_{47}O_{24}(OH)_{13}Cl_{25}(BO_3)_2(CO_3)$, with the carbonate and borate groups having independent structural sites inside the Pb oxo-hydroxo layers.

It is of interest that the synthetic iodine analogue of yeomanite, $Pb_2O(OH)I$, is monoclinic. The difference in the symmetry between synthetic $Pb_2O(OH)I$ and yeomanite can be assigned to the substitution of Cl^{-} by larger I^{-} anions. The $[O(OH)Pb_2]^{+}$ ribbons in $Pb_2O(OH)I$ are therefore unable to exist in perpendicular orientations due to the large I^{-} anions that prevent rotation of ribbons around their axes (Fig. 5). A similar influence of halogen atoms on the symmetry of Pb oxyhalides has been observed previously for Pb-La oxyhalides (Siidra *et al.*, 2007).

Yeomanite from the Kunibert Mine, Germany

While working on the type material of yeomanite, our wider study of Pb-oxychlorides from other localities continued, and in that work a minute amount of a fibrous phase was found on a specimen from the Kunibert mine in Rhine-Westphalia, Germany. We have now confirmed that this too is yeomanite. This investigation was also hampered by the small amount of material available, along with the fibrous nature of yeomanite.

Additionally, when the bright pink 'unknown oxychloride' described from the Kunibert mine by Rouse and Dunn (1990) was studied, surprisingly we found that the unit-cell parameters are identical to those of mereheadite (Krivovichev *et al.*, 2009). The cause of the unusual bright pink colouration is currently unknown – mereheadite from the type locality is invariably yellow-brown to orange-brown in colour.

It is therefore now clear that there are a number of close similarities between the mineralogy of the Kunibert mine and that of Merehead Quarry, including the presence of the rare Pb-oxyhalide minerals mendipite, mereheadite and now yeomanite.

Acknowledgements

The authors thank Dmitry Chernyshov (ESRF, Grenoble) for collecting synchrotron diffraction data for yeomanite crystals, which, unfortunately did not provide any improvement. This work was supported by St. Petersburg State University through the internal grant 3.38.238.2015, RFBR 15-35-20632, Russian Presidents grant MK-3756.2014.5. Technical support by the SPbSU X-Ray Diffraction Resource Center is gratefully acknowledged.

References

Brese, N.E. and O'Keeffe, M. (1991) Bond-valence parameters for solids. *Acta Crystallographica*, **B47**, 192–197.

https://doi.org/10.1180/minmag.2015.079.5.14 Published online by Cambridge University Press

Cooper, M.A. and Hawthorne, F.C. (1995) Diaboleite, $Pb_2Cu(OH)_4Cl_2$, a defect perovskite structure with stereoactive lone-pair behavior of Pb^{2+}. *The Canadian Mineralogist*, **33**, 1125–1129.

Cooper, M.A. and Hawthorne, F.C. (1999) The structure topology of sidpietersite, $Pb_4^{2+}S^{6+}O_3S^{2-}O_2(OH)_2$, a novel thiosulfate structure. *The Canadian Mineralogist*, **37**, 1275–1282.

Krivovichev, S.V. and Brown, I.D. (2001) Are the compressive effects of encapsulation an artifact of the bond valence parameters? *Zeitschrift für Kristallographie*, **216**, 245–247.

Krivovichev, S.V., Turner, R., Rumsey, M.S., Siidra, O.I. and Kirk, C.A. (2009) The crystal structure and chemistry of mereheadite. *Mineralogical Magazine*, **73**, 103–11.

Krivovichev, S.V., Mentré, O., Siidra, O.I., Colmont, M. and Filatov, S.K. (2013) Anion-centered tetrahedra in inorganic compounds. *Chemical Reviews*, **113**, 6459–6535.

le Page, Y. (1987) Computer derivation of the symmetry elements implied in a structure description. *Journal of Applied Crystallography*, **20**, 264–269.

Merlino, S., Pasero, M., Perchiazzi, N. and Gianfagna, A. (1995) X-ray and electron diffraction study of penfieldite: average structure and multiple cells. *Mineralogical Magazine*, **59**, 341–347

Rouse, R.C. and Dunn, P.J. (1990). A new lead sulphate oxychloride related to the nadorite group from Brilon, Germany. *Neues Jahrbuch fur Mineralogie Monatshefte*, **1990**, 337–342.

Rumsey, M.S. (2008) The First British occurrence of Kombatite; $Pb_{14}[O_9(VO_4)_2Cl_4]$ from the Wesley Mine near Westbury on Trym, Bristol. *Journal of the Russell Society*, **11**, 51–53.

Rumsey, M.S., Krivovichev, S.V., Siidra, O.I., Kirk, C.A., Stanley, C.J. and Spratt, J. (2011) Rickturnerite, $Pb_7O_4[Mg(OH)_4](OH)Cl_3$, a complex new Pb oxychloride mineral. *Mineralogical Magazine*, **76**(1), 59–73.

Siidra, O.I., Krivovichev, S.V., Armbruster, T. and Depmeier, W. (2007) Lead rare-earth oxyhalides: syntheses and characterization of Pb_6LaO_7X (X = Cl, Br). *Inorganic Chemistry*, **46**, 1523–1525.

Siidra, O.I., Krivovichev, S.V., Turner, R.W. and Rumsey, M.S. (2008) Chloroxiphite $Pb_3CuO_2(OH)_2Cl_2$ structure refinement and description in terms of oxocentered OPb_4 tetrahedra. *Mineralogical Magazine*, **72**, 793–798.

Siidra, O.I., Krivovichev, S.V., Turner, R.W., Rumsey, M. S. and Spratt, J. (2013*a*) Crystal chemistry of layered Pb oxychloride minerals with PbO-related structures. I. Crystal structure of hereroite, $[Pb_{32}O_{20}(O,\square)](AsO_4)_2((Si,As,V,Mo)O_4)_2Cl_{10}$. *American Mineralogist*, **98**, 248–255.

Siidra, O.I., Krivovichev, S.V., Turner, R.W., Rumsey, M. S. and Spratt, J. (2013*b*) Crystal chemistry of layered Pb oxychloride minerals with PbO-related structures. II. Crystal structure of vladkrivovichevite, $[Pb_{32}O_{18}][Pb_4Mn_2O]Cl_{14}(BO_3)_8{\cdot}2H_2O$. *American Mineralogist*, **98**, 256–261.

Siidra, O.I., Zenko, D.Y. and Krivovichev, S.V. (2013*c*). Crystal structure of novel synthetic compound $Pb_2O(OH)I$ and structure refinement of 'iodolaurionite', Pb(OH)I: hydroxo- and oxocentered units in Pb minerals and synthetic compounds. *Mineralogical Magazine*, **77**, 3239–3248.

Spek, A.L. (2003) Single-crystal structure validation with the program PLATON. *Journal of Applied Crystallography*, **36**, 7–13.

Spencer, L.J. and Mountain, E.D. (1923) New lead-copper minerals from the Mendip Hills, Somerset. *Mineralogical Magazine*, **20**, 67–92.

Turner, R.W. (2006) A mechanism for the formation of the mineralised manganese deposits at Merehead Quarry, Cranmore, Somerset, England. *Mineralogical Magazine*, **70**, 629–653.

Turner, R.W. and Rumsey, M.S. (2010) Mineral Relationships in the Mendip Hills. *Journal of the Russell Society*, **13**, 3–47.

Turner, R.W., Siidra, O.I., Rumsey, M.S., Krivovichev, S. V., Stanley, C.S. and Spratt, J. (2012*a*). Hereroite and vladkrivovichevite – two novel lead oxychlorides from the Kombat mine, Namibia. *Mineralogical Magazine*, **76(4),** 883–890.

Turner, R.W., Siidra, O.I., Krivovichev, S.V., Stanley, C.S. and Spratt, J. (2012*b*): Rumseyite, $[Pb_2OF]Cl$, the first naturally occurring fluoroxychloride mineral with the parent crystal structure for layered lead oxychlorides. *Mineralogical Magazine*, **76**(5), 1247–1255.

Venetopoulos, C.C. and Rentzeperis, P.J. (1975) The crystal structure of laurionite, Pb(OH)Cl. *Zeitschrift für Kristallographie*, **141**, 246–259.

Welch, M.D. and Lepore, G.O. (2010). The crystal structure of parkinsonite, nominally $Pb_7MoO_9Cl_2$: a naturally occurring Aurivillius phase. *Mineralogical Magazine*, **74**, 269–275.

Welch, M.D., Criddle, A.J. and Symes, R.F. (1998) Mereheadite, $Pb_2O(OH)Cl$: a new litharge-related oxychloride from Merehead Quarry, Cranmore, Somerset. *Mineralogical Magazine*, **62**, 387–393.

Welch, M.D., Cooper, M.A., Hawthorne, F.C. and Criddle, A.J. (2000) Symesite, $Pb_{10}(SO_4)O_7Cl_4(H_2O)$, a new PbO-related sheet mineral: description and crystal structure. *American Mineralogist*, **85**, 1526–1533.

Williams, P.A., Hatert, F., Pasero, M. and Mills, S.J. (2012) Plumbonacrite, IMA 11-G. CNMNC Newsletter 14, October 2012, page 1288. *Mineralogical Magazine*, **76**, 1281–1288.

https://doi.org/10.1180/minmag.2015.079.5.14 Published online by Cambridge University Press